

## Sondrestrom and EISCAT radar observations of poleward-moving auroral forms

R. M. ROBINSON,\* C. R. CLAUER,† O. DE LA BEAUJARDIERE,‡ J. D. KELLY,‡  
E. FRIIS-CHRISTENSEN§ and M. LOCKWOOD||

\*Space Sciences Laboratory, Lockheed Palo Alto Research Laboratory, Palo Alto, CA 94304, U.S.A.;

†STAR Laboratory, Stanford University, Stanford, CA 94305, U.S.A.; ‡Geoscience and Engineering Center, SRI International, Menlo Park, CA 94025, U.S.A.; §Division of Geophysics, Meteorologisk Institut, Copenhagen, Denmark; ||Rutherford Appleton Laboratory, Chilton, Didcot OX11 0QX, U.K.

(Received in final form 17 April 1990)

**Abstract**—During many magnetospheric substorms, the auroral oval near midnight is observed to expand poleward in association with strong negative perturbations measured by local ground magnetometers. We show Sondrestrom and EISCAT incoherent scatter radar measurements during three such events. In each of the events, enhanced ionization produced by the precipitation moved northward by several degrees of latitude within 10–20 min. The electric fields measured during the three events were significantly different. In one event the electric field was southward everywhere within the precipitation region. In the other two events a reversal in the meridional component of the field was observed. In one case the reversal occurred within the precipitation region, while in the other case the reversal was at the poleward boundary of the precipitation. The westward electrojet that produces the negative  $H$ -perturbation in the ground magnetic field has Hall and Pedersen components to varying degrees. In one case the Hall component was eastward and the Pedersen component was westward, but the net magnetic  $H$ -deflection on the ground was negative. Simultaneous EISCAT measurements made near the dawn meridian during one of the events show that the polar cap boundary moved northward at the same time as the aurora expanded northward at Sondrestrom. Most of the differences in the electrodynamic configuration in the three events can be accounted for in terms of the location at which the measurements were made relative to the center of the auroral bulge.

### INTRODUCTION

Because of the global nature of ionospheric effects produced in association with magnetospheric substorms, co-ordinated measurements obtained simultaneously at different locations are essential for a proper understanding of these processes. During the past several years there have been considerable efforts made in co-ordinating substorm observations, as evidenced by the success of programs such as PROMIS (HONES, 1985), MITHRAS (DE LA BEAUJARDIERE *et al.*, 1983) and GISMOS (DE LA BEAUJARDIERE, 1987). The data used in these studies include measurements obtained by satellite-borne detectors and ground-based instruments such as all-sky cameras, magnetometers and radars.

Incoherent scatter radars have contributed a wealth of information to these programs, particularly with regard to the ionospheric effects of substorms. They can measure variations in the electric fields and ionization produced by the substorm-associated particle precipitation. Radar measurements of substorm effects have been reported by DE LA BEAUJARDIERE *et*

*al.* (1988), RICHMOND *et al.* (1988), LOCKWOOD *et al.* (1988, 1989), CLAUER *et al.* (1989) and FOSTER *et al.* (1989). These studies include observations made by the Sondrestrom, EISCAT and Millstone Hill radars.

In this paper we report observations of substorm-associated aurora made by the Sondrestrom and EISCAT radars. The observations described here were made during times when auroral precipitation was expanding poleward to latitudes greater than 70°. Poleward-expanding aurora produces a distortion in the auroral oval boundary near midnight that is characteristic of many substorms. According to the phenomenological model of substorms developed by AKASOFU (1976), magnetospheric substorms begin with the activation of auroral arcs near midnight. The active region expands rapidly poleward and away from midnight toward the dawn and dusk meridians. This active region is often referred to as the auroral bulge. For an observer situated poleward of the auroral oval before the substorm, the bulge is associated with the sudden appearance of intense aurora. Near midnight, the bright aurora is seen to move into the field-of-view from lower latitudes in the south. Dusk-

ward or dawnward of the midnight sector the aurora appears to move in from the east or west, respectively. The westward propagating aurora observed in the pre-midnight hours is referred to as a westward travelling surge.

Although many observations of substorms have been made from invariant latitudes between 60 and 70°, there have been few studies of electric fields and currents associated with that part of the substorm-associated aurora that expands poleward near local midnight. This is because there are few observing sites at the very high latitudes required to make such observations. In this paper we describe observations of poleward-expanding auroral forms made near 74° invariant latitude using the Sondrestrom incoherent scatter radar. Each event is characterized by the rapid appearance of aurora from southern latitudes accompanied by a distinct negative bay in the ground-based magnetometer *H*-component. We show data from three events. One of these events occurred during simultaneous operation of the Sondrestrom and EISCAT radars as part of the GISMOS program. These data are used to examine the extent in local time of the effects associated with the substorms.

We begin with a brief description of the two radar facilities. We then describe the data obtained during the three events. Ground-based magnetometer data from Sondre Stromfjord are used to determine the dynamic behavior of the electrojets during the experiments. Finally, we discuss the results in terms of the location at which each of the observations was made relative to the large-scale substorm morphology.

#### RADAR OBSERVATIONS

The data shown here were obtained from the Sondrestrom and EISCAT incoherent scatter radars and the Greenland chain of ground-based magnetometers. The Sondrestrom and EISCAT radars are described by KELLY (1983) and RISHBETH and WILLIAMS (1985), respectively. Both are able to measure ion drifts, electron densities, electron and ion temperatures and a number of other ionospheric and thermospheric properties. The antennae are steerable, allowing a great deal of flexibility in designing antenna scan patterns to meet specific observational requirements.

The Sondrestrom radar is located at an invariant latitude of 74° and is usually poleward of the quiet auroral oval on the nightside, where most substorm effects are easily observable. At Sondrestrom, magnetic midnight is at about 0200 UT. The radar measurements described here were made while the antenna was scanning within the magnetic meridian

plane. These scans took 5 min to complete and extended from approximately 25° elevation in the south to 25° in the north. In one of the experiments, these scans are interspersed with fixed position measurements in the north and south to extend the electric field measurements to more distant latitudes.

The EISCAT measurements shown here were obtained using the POLAR mode (VAN EYKEN *et al.*, 1984; WILLIS *et al.*, 1986). In this mode the radar makes measurements for 2 min at each of two azimuths 12° on each side of magnetic north. The elevation angle of the antenna is 21.5°, which allows measurements to be obtained at invariant latitudes between 70 and 75°. For this EISCAT field-of-view, magnetic midnight occurs at about 2130 UT so that the measurements are made about 4.5 h of local time east of Sondrestrom.

The Greenland magnetometer array is described by FRIIS-CHRISTENSEN *et al.* (1985). Only the data from Sondre Stromfjord are shown here, and we confine ourselves to the *H*- and *Z*-component variations which allow a qualitative determination of the dynamic behavior of the east-west ionospheric currents. Data from three of the substorm events are shown in Fig. 1. The substorm events are identified by the sudden decrease in the *H*-component of the Sondre Stromfjord magnetometer. Above the *Z*-trace in each panel are arrows that indicate the times of Sondrestrom elevation scans, for which the data are presented below.

#### RESULTS

##### 18 November 1985

The magnetometer data for the 18 November event are shown in the top panel of Fig. 1. There is a small negative bay at about 2200 UT, but here we will concentrate on the more intense event at 2300 UT. The negative *H*-perturbation was about 200 nT and the variations in the *Z*-component indicate that the westward electrojet moved poleward from a location equatorward of Sondre Stromfjord and passed over the station at about 2300 UT.

The electron densities measured during the Sondrestrom radar elevation scans are shown in Fig. 2. The contour plots show the electron density in the magnetic meridian plane between 80 and 200 km altitude. The horizontal scale is invariant latitude so that the data have been rearranged with magnetic field lines exactly vertical. The first scan in the sequence shows the state of the ionosphere before the event, with electron densities generally below  $4 \times 10^{10} \text{ m}^{-3}$ . The data from the next scan show that within a time

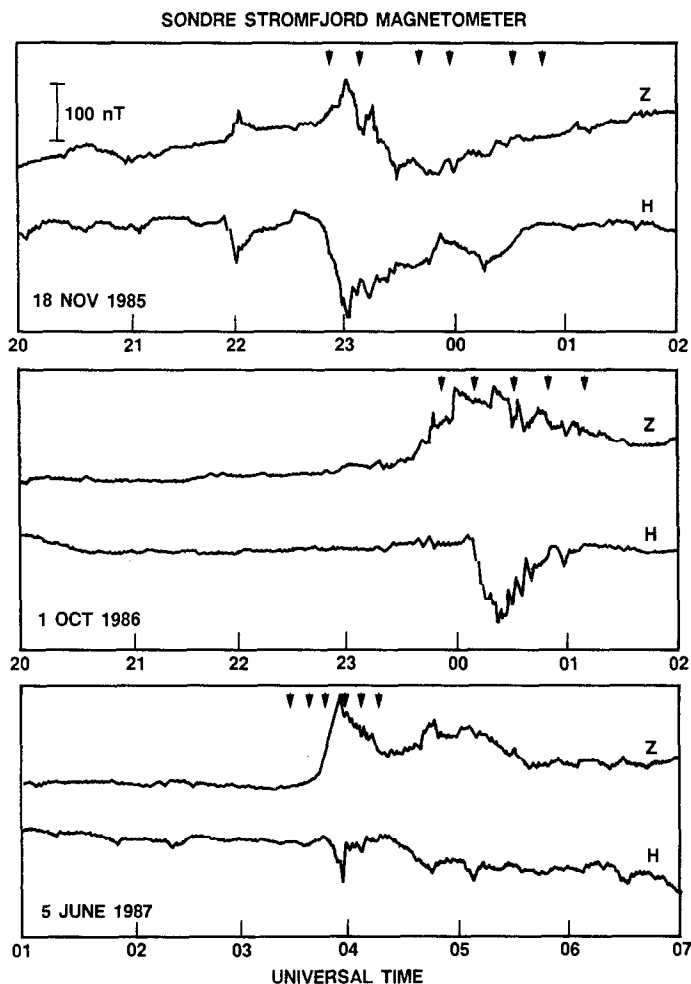


Fig. 1.  $H$  and  $Z$  magnetic perturbations measured during three poleward-expanding auroral events at Sondrestromfjord. The arrows show the times of elevation scans for which electron density data are shown in subsequent figures.

of about 10 min a widespread region of fairly intense aurorally produced ionization appeared overhead. Because this correlates well with the decrease in the magnetometer  $H$ -component and the increase in the  $Z$ -component, it is likely that the aurora was coincident with the poleward-moving westward electrojet. Note that the precipitation producing the poleward expanding aurora is highly dynamic and typically consists of several rayed arcs with both large- and small-scale loops and folds. Because the antenna scan is relatively slow the electron densities shown in these plots do not represent the instantaneous distribution of ionization in the meridian plane. The data from consecutive scans show that the aurora remained over

the station for about 1.5 h, after which the arcs disappeared and the ionosphere recovered to its previous state. Note that elevation scans were also made beginning at 2322 and 0009 UT, but the contour plots are not shown here.

Ion drift velocities measured during this event are shown in vector format in Fig. 3. Each vector is plotted with its origin at the UT and invariant latitude at which the measurement was made. The numbers below each set of vectors refer to the scans in Fig. 2 during which the measurements were obtained. In the elevation scan mode, the vector electric field is determined by combining  $E$ -region and  $F$ -region velocity measurements (see DE LA BEAUJARDIERE *et al.*,

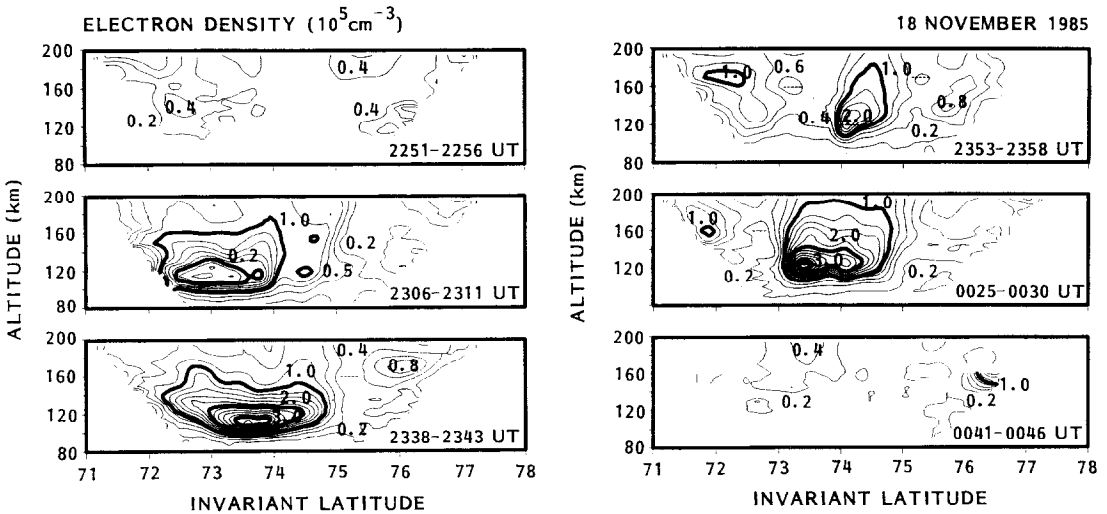


Fig. 2. Electron density contour plots constructed from Sondrestrom meridian scan measurements made during the 18 November 1985 event. Magnetic field lines are vertical in these displays.

1977). Because of the low *E*-region electron densities prior to the onset of the aurora, the drift measurements made during the first scan have large uncertainties and are not shown. The measurements made after the event show that the appearance of the aurora was accompanied by electric fields that were primarily southward, producing eastward ion drifts. The southward electric fields in the presence of the enhanced ionospheric conductance produce the westward elec-

trojet current measured by the ground magnetometers.

*1 October 1986*

Data from a similar event were obtained on 1 October 1986. The magnetometer data (Fig. 1) show that the *H*-component of the ground magnetic field began to decrease suddenly at about 0010 UT, although the *Z*-component increased prior to this time. This again indicates poleward motion of a region of westward ionospheric current. Figure 4 shows electron densities measured during this event. As in the 18 November event, the auroral ionization appears within the 15 min interval between the first two scans shown. The ionization reaches its most poleward extent at about 0030 UT, then recedes slowly southward again. For this experiment, scans were made every 10 min so that contour plots are only shown for every other scan.

The vector drift measurements for this event are shown in Fig. 5. In contrast to the 18 November event, the drifts during this event are southward. The westward component of this drift results from a northward electric field which drives an eastward current. This eastward Hall current, however, is exceeded by the westward Pedersen current driven by the westward electric field. Thus, the Pedersen currents produce the negative bay seen in the ground magnetometer data. In Fig. 5, velocities that have components toward magnetic east are shown as heavy lines, while those

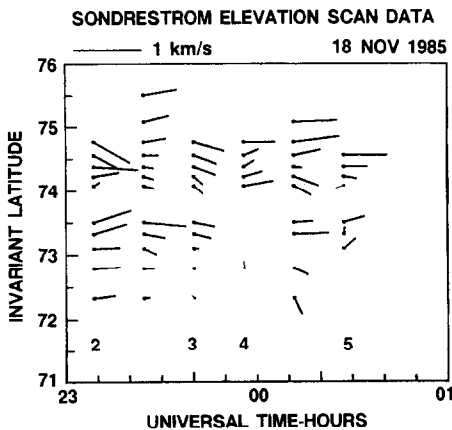


Fig. 3. Vector plasma drifts measured during the Sondrestrom meridian scans on 18 November. The numbers on the bottom indicate which of the six scans shown in Fig. 2 the measurements were obtained from.

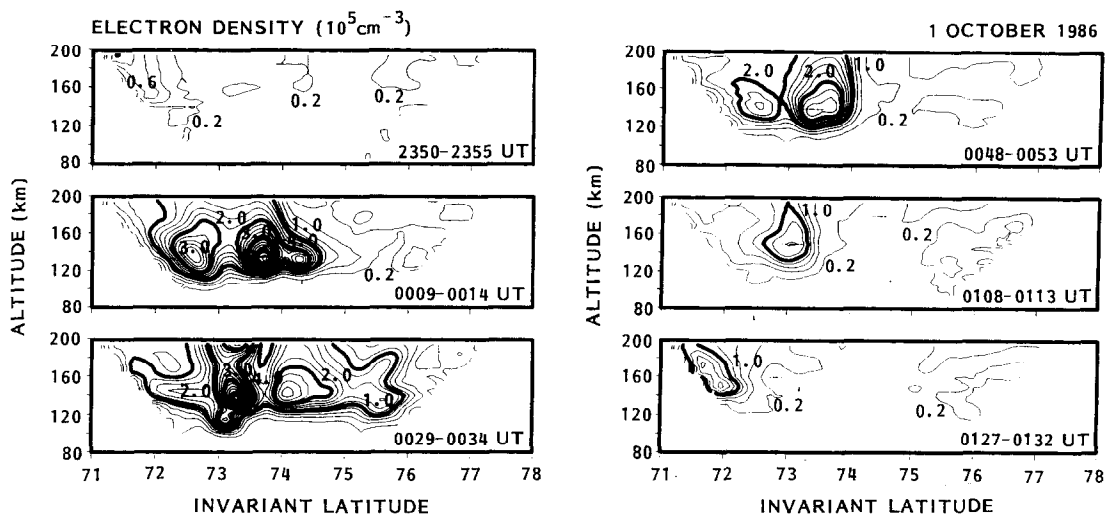


Fig. 4. Electron density contour plots constructed from Sondrestrom meridian scan measurements made during the 1 October 1986 event. Magnetic field lines are vertical in these displays.

that have components toward magnetic west are shown by thin lines. There is some evidence for a reversal in the east–west component of the drifts at the lower latitudes.

#### 5 June 1987

The third event described here occurred during the June 1987 GISMOS campaign, and simultaneous measurements are available from both the Sondrestrom and EISCAT radars. Various aspects of this

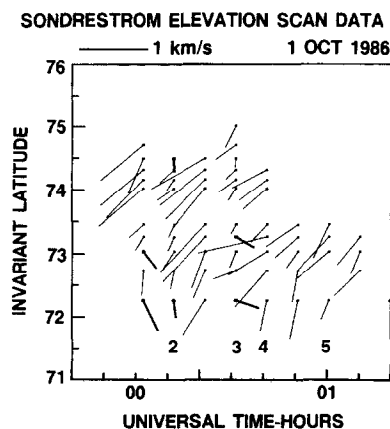


Fig. 5. Vector plasma drifts measured during the Sondrestrom meridian scans on 1 October. The numbers on the bottom indicate which of the six scans shown in Fig. 4 the measurements were obtained from.

event have been described by LOCKWOOD *et al.* (1988, 1989) and CLAUER *et al.* (1989). The magnetometer data in Fig. 1 show that the negative bay occurred at about 0345 UT, or 0145 MLT at Sondrestrom. Note that the  $Z$ -perturbation remains positive and is larger than the  $H$ -perturbation, indicating that the center of the westward electrojet remained equatorward of Sondre Stromfjord throughout the event. This is consistent with the results shown in the electron density contour plots of Fig. 6. In the first two panels, aurorally produced ionization is absent and the radar observes the ionosphere poleward of the auroral oval. Within 5 min, between 0341 and 0346 UT, the aurora moves poleward so that it can be seen in the southern portion of the radar field-of-view at invariant latitudes less than  $73^\circ$ . It remains at this location for about 30 min before receding equatorward again. This time interval corresponds to the duration of the negative  $H$ -event in the ground magnetometer data.

Ion drift velocity vectors are shown in Fig. 7. Because fixed position measurements were made between the meridian scans, vector velocity data are also available from higher and lower latitudes than shown in the previous two experiments. In Fig. 7, we show data for about 3 h before the event to establish the general nature of the convection present. As in Fig. 5, we use thin or heavy lines to denote vectors with westward or eastward components, respectively. Prior to 0330 UT a reversal in the convection flow can be seen at latitudes below about  $70^\circ$ . The westward flow poleward of this boundary indicates the presence

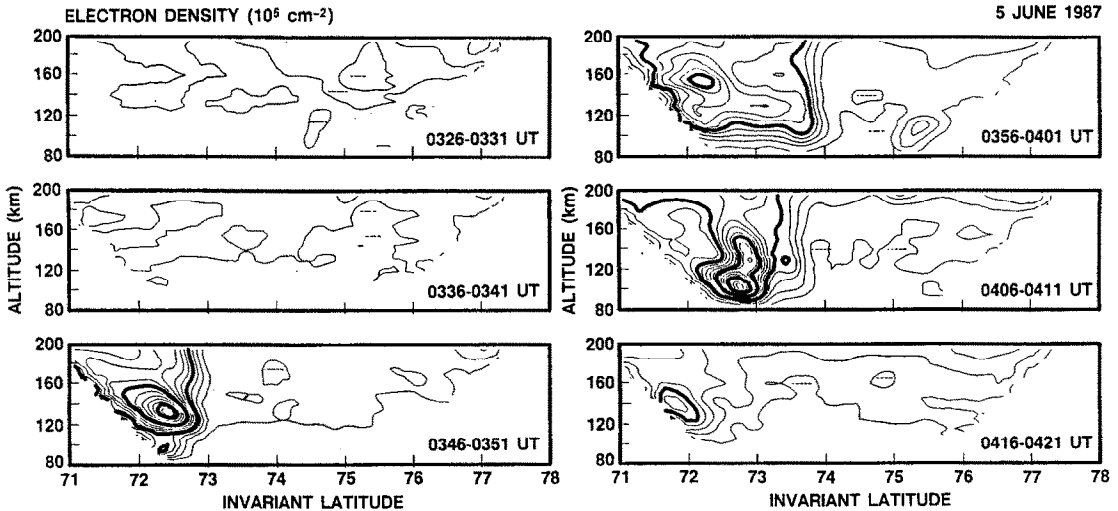


Fig. 6. Electron density contour plots constructed from Sondrestrom meridian scan measurements made during the 5 June 1987 event. Magnetic field lines are vertical in these displays.

of a southward electric field at high latitudes within the polar regions. Between 0330 UT and 0350 UT, the region of eastward convection in the south moves poleward so that the convection reversal is situated near  $74^\circ$  latitude. There is also evidence for an increase in the equatorward component of the drift. Note that the direction of motion of the convection reversal boundary is opposite to the direction of plasma drift.

The heavy line in Fig. 7 indicates the poleward extent of the *E*-region ionization enhancement associated with the auroral precipitation. This poleward edge of the precipitation region coincides with the convection reversal boundary during the poleward expansion.

This electric field configuration may be contrasted to that observed at EISCAT located near dawn. The vector ion drifts over a 2-h time interval are shown in

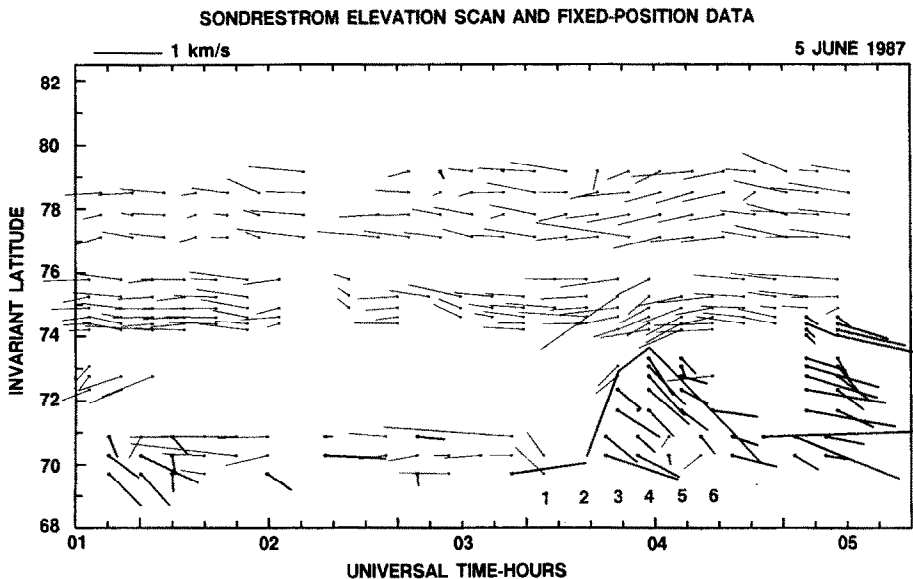


Fig. 7. Vector plasma drifts measured during the Sondrestrom meridian scans on 5 June. The numbers on the bottom indicate which of the six scans shown in Fig. 6 the measurements were obtained from. The heavy line shows the poleward extent of *E*-region ionization measured during the event.

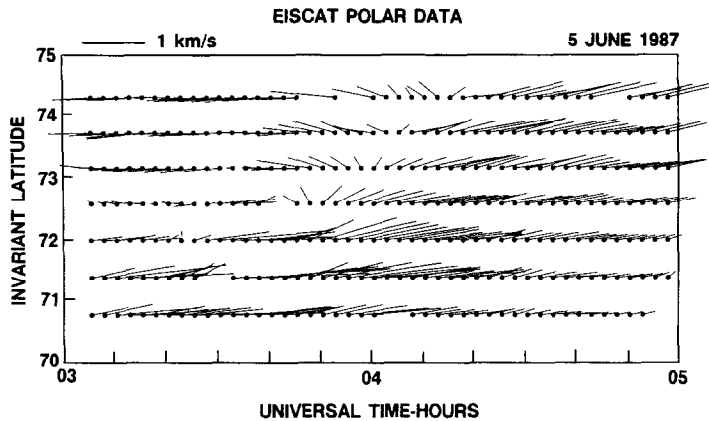


Fig. 8. Vector plasma drifts measured during the EISCAT POLAR experiments on 5 June 1987.

Fig. 8. Prior to 0330 UT there is a convection reversal at  $73^\circ$  in the same sense as that seen at Sondrestrom. The first indication of a change in the convection occurs at 0350 UT, when there is an increase in the poleward component of drift, or eastward electric field. This clockwise rotation continues until the plasma flow is predominantly in the eastward direction. The time at which the rotation to eastward drift occurs is later at higher latitudes. LOCKWOOD *et al.* (1988) have presented a detailed analysis of these variations in drift along with the associated changes in plasma temperature and density. By modeling the expected line-of-sight drift velocities they show that this pattern can be produced by the poleward propagation of a region of shear reversal. In general, the motion of the boundary does not correspond to the motion of the plasma within the expanding bulge.

#### DISCUSSION

The Sondrestrom and EISCAT data presented here reveal several important properties pertaining to the precipitation and electric fields in the high latitude ionosphere during times when substorm-associated aurora is expanding poleward. Each of the three events was associated with enhanced *E*-region ionization produced by intense precipitation and accompanied by a negative *H*-component magnetic perturbation. However, the electric field configuration in each of the three events is different.

For the 18 November event, *E*-region electron densities prior to the event were less than  $1 \times 10^{10} \text{ m}^{-3}$  and accurate measurements of the vector electric field could not be made. During the event, the electric field was primarily southward producing eastward drifts

up to  $700 \text{ m s}^{-1}$ . The magnetic local time of the event spanned the interval from 2100 to 2230, so that Sondrestrom was in the evening sector. In the evening sector, the normal auroral zone convection is westward, while in the polar cap it is generally southward. Thus, the observed southward electric field probably represents a local disturbance in the quiet-time convection. The observed change cannot easily be explained in terms of motion of a boundary.

The electric fields observed during the 1 October event are significantly different. As above, the fields prior to the event could not be measured accurately. During the event the drifts have both southward and westward components, indicating northwestward electric fields. As shown in Fig. 5, the drifts near the poleward regions of the radar field-of-view are southwestward, while at lower latitudes the drifts are predominantly southward. There is also evidence for a temporal variation in the fields. In some scans the drifts are larger than those measured in others. This suggests that the temporal variations affect the electric fields over extended regions of the ionosphere.

The event that occurred on 5 June shows another possible configuration of electric fields associated with poleward-moving aurora. This was a summer event and the ambient ionization was high enough to allow measurement of the electric field prior to the event. In addition, fixed position measurements made between the meridian scans provide measurements of electric fields at higher and lower latitudes. In Fig. 7 the westward drift poleward of  $74^\circ$  is probably associated with polar cap convection. Interplanetary magnetic field (IMF) data from IMP-8 for this event show that the *y*-component of the IMF was positive throughout the event. For a positive IMF  $B_y$ , the statistical study of

drifts performed by DE LA BEAUJARDIERE *et al.* (1986) shows that there is a convection cell centered in the early morning local time sector. The sense of rotation in this cell is westward on the poleward side and eastward on the equatorward side. Some evidence for this eastward drift is evident in the data from 5 June at latitudes below  $71^\circ$ . At the start of the event (approximately 0345 UT), the zone of eastward flowing plasma appears to move poleward, so that between 0400 and 0500 UT there is a well-defined flow reversal near  $74^\circ$  latitude. As shown in Fig. 7, this flow reversal is collocated with the poleward boundary of the precipitation region. In this case, the difference between the electric field configuration before and after the event can be explained by motion of the convection reversal boundary with no inherent temporal variation in the field itself. This has been interpreted to be a contraction of the polar cap, and the equatorward flows observed in the precipitation region are interpreted to be the flow out of the polar cap that is responsible for the contraction (CLAUER *et al.*, 1989).

The measurements made from Sondre Stromfjord give no indication about the local time variations across the poleward-expanding auroral forms. Fortunately, we can take advantage of simultaneous measurements made by the EISCAT radar during the 5 June event. The EISCAT data for this event have been described by LOCKWOOD *et al.* (1988, 1989). They show that the drifts measured by EISCAT during this event are consistent with the poleward motion of a convection reversal boundary. Unfortunately, the precipitation accompanying this motion of the boundary cannot be determined from the radar measurements because they are made at *F*-region altitudes. However, because the event occurred near the summer solstice, the *E*-region was sunlit and the conductances were enhanced through photoionization. Although no magnetometer data are available at the latitudes sampled in this operating mode, it is likely that the southwestward electric fields would drive a strong westward electrojet producing a negative *H*-deflection on the ground. Thus, there is good evidence that the negative bay associated with the poleward-moving aurora was extended in local time by at least 4 h toward the east. CLAUER *et al.* (1989) examined magnetometer data from several Canadian stations during this event and showed that the negative bay was also detected 4 h of local time to the west of Sondre Stomfjord. Although the magnetic effects associated with this event were observed over 8 h of local time, there is no evidence to indicate whether the enhanced precipitation was also extended over many hours of local time.

Figure 9 summarizes our results in terms of the

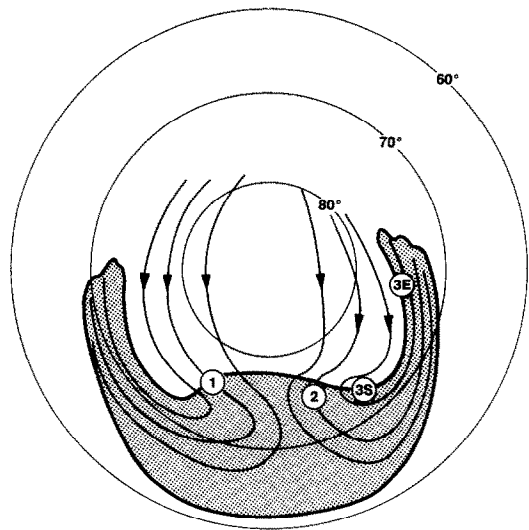


Fig. 9. Schematic illustration of the location at which the Sondrestrom and EISCAT radar observations were made for the three events. The midnight local time sector is at the bottom and dawn is to the right. The shaded region indicates auroral precipitation with the bulge at midnight representing the auroral forms that have expanded poleward from their pre-event location. Streamlines show plasma convection associated with the bulge. The circle labeled 1 is for the 18 November event, 2 is the 1 October event, and 3S and 3E indicate the Sondrestrom and EISCAT measurements for the 5 June event, respectively.

observed relationships between electric fields and precipitation associated with poleward-moving aurora. As in the model of AKASOFU (1976), the bulge in the midnight sector represents the expanded auroral precipitation region. The numbered circles correspond to the locations at which the Sondrestrom and EISCAT observations were made for the three events. The directions of the observed plasma drifts are indicated by the streamlines passing through the numbered circles. These streamlines have been extended from the observation points to form a two-cell convection pattern that might exist during the substorm events. Because the electric field configuration probably depends on the direction of the interplanetary magnetic field at the time of the poleward expansion, this sketch is not meant to be an instantaneous convection pattern. In particular, the *y*-component of the IMF may determine the direction from which polar cap plasma enters the bulge region. For the 5 June event, the *y*-component of the IMF was positive and there were strong westward drifts poleward of the auroral zone in the morning sector, as one would expect under these conditions. No IMF data are available for the other two events. However,

the westward convection observed on 1 October suggests that the  $y$ -component of the IMF may have been positive for this event also. For this reason, in Fig. 9 we have sketched the convection pattern such that these observations are placed in the dawn cell even though the actual magnetic local time was pre-midnight. The drifts observed on 18 November are more consistent with a pre-midnight configuration. An important difference in the electric fields measured in the 5 June event is that at Sondrestrom the convection reversal boundary coincides with the particle precipitation boundary. This can be contrasted with the 1 October event, where the convection reversal lies within the region of enhanced particle precipitation.

Because of the distinct electric field configurations observed on the three days, the source of the observed negative bay is different in each case. For 18 November, the westward electrojet is a Hall current driven by the southward electric fields. The maximum negative  $H$ -perturbation occurs at about 2300 UT when the electric fields measured by the radar are largest. The decrease in the magnitude of the negative  $H$ -perturbation is caused by a decrease in the electric field, particularly at latitudes less than  $74^\circ$ , where the ionization is most intense. For 1 October, the northward electric field component drives an eastward Hall current while the westward component of the field drives a westward Pedersen current. Because the net magnetic  $H$ -perturbation on the ground is negative, the westward Pedersen current must dominate. This is because the westward Pedersen current is situated closer to the Sondre Stromfjord zenith, while the eastward Hall current is farther to the north. The maximum  $H$ -perturbation occurs at 0020 UT when the westward component of the field is large. The decrease in the magnitude of this perturbation occurs as the aurora recedes equatorward. For 5 June, the westward electrojet is sustained by the south-westward electric field in the presence of the enhanced conductances. The negative  $H$ -perturbation in the magnetometer does not exceed 150 nT because the center of the electrojet never reaches the Sondre Stromfjord zenith. It is clear from the  $Z$ -component, however, that the electrojet is fairly intense. The maximum perturbation is observed at 0400 UT when the electric fields are largest and the perturbation decreases as the aurora moves equatorward.

The electrodynamic properties of substorm-associated aurora have been studied using an extensive variety of techniques. Most of the ground-based studies were made at invariant latitudes equatorward of  $70^\circ$  (see, for example, OPGENOORTH *et al.*, 1980, 1983; BAUMJOHANN *et al.*, 1981; INHESTER *et al.*, 1981). These observations have led to the development of

models for the electric fields and currents associated with auroral substorms. Some of these models have been the basis for theoretical models of westward traveling surges (ROTHWELL *et al.*, 1984; KAN and KAMIDE, 1985). However, a given substorm may be characterized by a westward traveling surge or poleward-expanding aurora, or some combination of both. In some cases it may be difficult to determine whether the sudden appearance of intense aurora at a given location is due to the westward propagation of a disturbance region or the poleward motion of pre-existing auroral forms from lower latitudes. For this reason the results presented here may not be directly comparable to previous studies that concentrate on break-up aurora and surges observed at latitudes below  $70^\circ$ .

## CONCLUSIONS

The data presented above show that a poleward-expanding aurora is a well-defined event at latitudes above  $70^\circ$ , consisting of intense precipitation and westward ionospheric currents. In all cases there is evidence for poleward motion of both the precipitation and the electrojet, and each event is characterized by the sudden onset of a negative bay in the ground magnetic  $H$ -component. However, apart from these features the electrodynamics of different events can be quite distinct. In one of the cases studied it is fairly clear that the electric field changed in a manner that could not be attributed to motion of a boundary. In the other two cases, the convection reversal boundary that moved poleward during the event may have been present at lower latitudes before the event. Because of the different electric field patterns, the ionospheric currents are also different. In one case the westward electrojet was a Hall current driven by southward electric fields, while in another case the westward electrojet was a Pedersen current. The Pedersen current for this event opposes the Hall component of the current because the meridional electric field was northward. These differences are undoubtedly related to the location of the measurements relative to the center of the expanding bulge. As we have shown that some ionospheric effects associated with poleward-expanding aurora can span many hours of local time, co-ordinated measurements at different locations are essential for understanding the electrodynamic properties of these events.

*Acknowledgements*—We thank the site crew of the Sondrestrom radar for their assistance in operating the radar during these experiments. This work was supported at

Lockheed by National Science Foundation grant ATM-8717840 and the Lockheed Independent Research Program. At SRI International, research with the Sondrestrom radar is supported by National Science Foundation grant ATM-8822560 and Air Force Office of Scientific Research contract F49620.87K7. Support to Stanford University for this research has been provided by the National Science Foundation through grant ATM-8800327.

## REFERENCES

- AKASOFU S.-I. 1976 *Space Sci. Rev.* **19**, 169.
- BAUMJOHANN W., PELLINEN R. J., OPGENOORTH H. J. and NIELSEN E. 1981 *Planet. Space Sci.* **29**, 431.
- BEAUJARDIERE O. DE LA 1987 *EOS Trans. Amer. Geophys. Union* **68**, 483.
- BEAUJARDIERE O. DE LA, EVANS D., KAMIDE Y. and LEPPING R. 1988 *Magnetosphere-Ionosphere Plasma Models*, MOORE and WAITE (eds). American Geophysical Union, Washington, D.C.
- BEAUJARDIERE O. DE LA, HOLT J. and NIELSEN E. 1983 *Radio Sci.* **18**, 981.
- BEAUJARDIERE O. DE LA, VONDRAK R. and BARON M. 1977 *J. geophys. Res.* **82**, 5051.
- BEAUJARDIERE O. DE LA, WICKWAR V. and KING J. 1986 *Solar Wind-Magnetosphere Coupling*, KAMIDE and SLAVIN (eds). Terra/Reidel, Tokyo.
- CLAUER C. R., KELLY J. D., LOCKWOOD M., ROBINSON R. M., RUOHONIEMI J. M., BEAUJARDIERE O. DE LA and HAKKINEN L. 1989 *Adv. Space Res.* **9**(5), 29.
- EYKEN A. P. VAN, RISHBETH H., WILLIS D. M. and COWLEY S. W. H. 1984 *J. atmos. terr. Phys.* **46**, 635.
- FOSTER J. C., TURUNEN T., POLLARI P., KOHL H. and WICKWAR V. B. 1989 *Adv. Space Res.* **9**(5), 19.
- FRIIS-CHRISTENSEN E., KAMIDE Y., RICHMOND A. D. and MATSUSHITA S. 1985 *J. geophys. Res.* **90**, 1325.
- HONES E. 1985 *EOS Trans. Amer. Geophys. Union* **66**, 1369.
- INHETER B., BAUMJOHANN W., GREENWALD R. A. and NIELSEN E. 1981 *J. Geophys.* **49**, 155.
- KAN J. R. and KAMIDE Y. 1985 *J. geophys. Res.* **90**, 7615.
- KELLY J. D. 1983 *Geophys. Res. Lett.* **10**, 1112.
- LOCKWOOD M., COWLEY S. W. H., CLAUER C. R., TODD H., CROTHERS S. R. and WILLIS D. M. 1989 *Adv. Space Res.* **9**(5), 39.
- LOCKWOOD M., COWLEY S. W. H., TODD H., WILLIS D. M. and CLAUER C. R. 1988 *Planet. Space Sci.* **36**, 1229.
- OPGENOORTH H. J., PELLINEN R. J., BAUMJOHANN W., NIELSEN E., MARKLUND G. and ELIASSON L. 1983 *J. geophys. Res.* **88**, 3138.
- OPGENOORTH H. J., PELLINEN R. J., MAURER H., KUPPERS F., HEIKKILA W. J., KAILA K. U. and TANSKANEN P. 1980 *J. Geophys.* **48**, 101.
- RICHMOND A. D., KAMIDE Y., AHN B.-H., AKASOFU S.-I., ALCAYDE D., BLANC M., BEAUJARDIERE O. DE LA, EVANS D. S., FOSTER J. C., FRIIS-CHRISTENSEN E., FULLER-ROWELL T. J., HOLT J. M., KNIPP D., KROEHL H., LEPPING R. P., PELLINEN R. J., SENIOR C. and ZAITSEV A. N. 1988 *J. geophys. Res.* **93**, 5760.
- RISHBETH H. and WILLIAMS P. J. S. 1985 *Q. Jl R. astr. Soc.* **26**, 478.
- ROTHWELL P. L., SILEVITCH M. B. and BLOCK L. P. 1984 *J. geophys. Res.* **89**, 8941.
- WILLIS D. M., LOCKWOOD M., COWLEY S. W. H., EYKEN A. P. VAN, BROMAGE B. J. I., RISHBETH H., SMITH P. R. and CROTHERS S. R.